A shape optimisation technique for the Wagner problem

Thomas GAZZOLA
Bureau Veritas - Research Department, École Centrale Paris, Paris, France, thomas.gazzola@centraliens.net

Wagner did introduce in 1932 a simplified model of great use to deal with fluid structure impacts [Wag32].

The two dimensional case has been extensively studied in the past (see *e.g.* [ZF93]); a variational inequality method has been introduced to solve the three dimensional Wagner impact [GKMS05].

One suggests in this chapter to use a shape optimisation process to deform the contact line Γ in order to determine the 3D Wagner contact line.

Introduction

It is suggested in [Kor82] to introduce the displacement potential ϕ, which is the integration with respect to time of the velocity potential φ.

$$\phi(\vec{x},t) = \int_0^t \varphi(\vec{x},\tau)\ d\tau. \tag{1}$$

Considering a structure f falling in flat water that occupies $z<0$, the Wagner approximation linearises the free and wet surfaces one the plan $\{z=0\}$. The gravity is neglected, leading to $\phi = 0$ on the free surface. On the wet surface, the fluid elevation is exactly the position of the structure.

The contact line is unknown. Anyway, for *any*[1] curve Γ defining a wet surface Γ_w and a free surface Γ_f, one can write a boundary value problem for the displacement potential.

$$\left\{\begin{array}{cl} \Delta\phi = 0 & \text{in } \Omega = \{z<0\} \\ \phi = 0 & \text{on } \Gamma_f \\ \partial_z\phi = f(\vec{x}) - h(t) & \text{on } \Gamma_w \\ \phi \to 0 & \text{in the far field,} \end{array}\right. \tag{2}$$

where h is the penetration depth of the entering body. One defines the bilinear laplacian form a, and the linear form l, from the Neumann condition.

$$a(u,v) = \int_\Omega \nabla u \cdot \nabla v \ \mathrm{d}\Omega, \tag{3}$$

$$l(v) = \int_{\Gamma_w} (f-h)\cdot v \ \mathrm{d}\Sigma. \tag{4}$$

The linear boundary value problem (2) can be reduced to the unconstrained minimisation of functional

$$J(\phi) = \frac{1}{2}a(\phi,\phi) - l(\phi). \tag{5}$$

[1] Not necessary the Wagner contact line, since it must be found.

The potential ϕ is the unique function which minimises J in the weighted Sobolev space

$$W^1(\Omega) = \left\{ v\ ;\ \frac{v}{\sqrt{1+|\vec{x}|^2}} \in L^2(\Omega) \text{ and } \frac{\partial v}{\partial x}, \frac{\partial v}{\partial y}, \frac{\partial v}{\partial z} \in L^2(\Omega) \right\}. \tag{6}$$

Justification of this results may be found in [GKMS05].

However, resolution of the boundary value problem (2) is not of *immediate* help, since the considered contact line Γ is *not* the Wagner contact line, which has to be found.

One wants to deform the curve Γ toward the Wagner contact line. In other words, the influence on the solution of BVP (2) of a variation of the wet surface is studied. More precisely, the variations of J with respect to Γ are evaluated.

In this paper, we establish a link between $\partial_\Gamma J$ and the Wagner problem. In particular, the asymptotic behaviour of the solution around the line Γ is linked to both $\partial_\Gamma J$ and the Wagner problem.

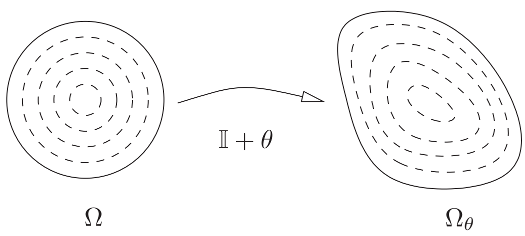

Figure 1: The domain Ω is transformed into Ω_θ

The derivation of J with respect to the contact line is performed using a domain derivation process. The foremost idea is to consider a vector field θ, and to deform the studied domain in the direction of θ. The effect of this transformation will lead to the directional derivative with respect to the domain.

The derivation of the laplacian symmetrical bilinear form on the *unbounded* fluid domain $\Omega = \{z<0\}$ will be computed. Its re-writing on the boundary $\{z=0\}$ will require special care because of the singular[2] behaviour of the potential next to the curve Γ. The derivative of J will then be linked to the behaviour of the solution ϕ. Then this behaviour will be linked to the Wagner problem.

Two-dimensional and three-dimensional examples are presented to illustrate the shape optimisation technique.

[2] The potential is singular in the sense where its derivative is unbounded.

1 Derivating with respect to the contact line

The used mathematical developments and justifications concerning shape optimisation are gathered together in [All06].

One considers the domain $\Omega = \{z < 0\}$. For every regular enough vector field θ, from $\mathbb{R}^n$ to $\mathbb{R}^n$ (n=2 or 3), we define Ω_θ as the image of Ω by $\mathbb{I}+\theta$.

$$\Omega_\theta = (\mathbb{I}+\theta)(\Omega), \tag{7}$$

where $\mathbb{I}$ is the identity application.

1.1 Derivating the bilinear form a

The main point to perform the derivation of the bilinear laplacian form a is to write it on the deformed domain. Using a change of variables will bring the derivative of a, after a first order expansion.

$$\begin{aligned} a^\theta(u^\theta, u^\theta) = \int_\Omega & ([\nabla(\mathbb{I}+\theta)]^{-1} \cdot \nabla u) \cdot \\ & ([\nabla(\mathbb{I}+\theta)]^{-1} \cdot \nabla v) \cdot \\ & det(\nabla(\mathbb{I}+\theta)) \, \mathrm{d}\Omega, \end{aligned} \tag{8}$$

where a θ exponent characterises what is defined on domain Ω_θ.

A first order development is used.

$$[\nabla(\mathbb{I}+\theta)]^{-1} = \mathbb{1} - \nabla\theta + o(\theta), \tag{9}$$

where $\mathbb{1}$ is the constant identity matrix. The Jacobian of the transformation is $\mathbb{1} + \nabla\theta$, and the first order Taylor expansion of its determinant is

$$det(\mathbb{1} + \nabla\theta) = 1 + div(\theta) + \|o(\theta)\|. \tag{10}$$

In order to obtain a first order development of bilinear form a^θ, we substitute equations (9) and (10) into equation (8).

$$\begin{aligned} a^\theta(u^\theta, u^\theta) = & \int_\Omega \nabla u \cdot \nabla v \, \mathrm{d}\Omega \\ & + \int_\Omega \nabla u \cdot [div(\theta) \cdot \mathbb{1} - \nabla\theta - {}^t\nabla\theta] \cdot \nabla v \, \mathrm{d}\Omega \\ & + \|o(\theta)\|. \end{aligned} \tag{11}$$

The leading order appears to be the laplacian bilinear form a written on the undeformed domain Ω. Hence the derivative a' of the bilinear form a, with respect to the domain Ω, in the direction θ, may be defined as

$$a'(u,v)(\theta) = \int_\Omega \nabla u \cdot [div(\theta) \cdot \mathbb{1} - \nabla\theta - {}^t\nabla\theta] \cdot \nabla v \, \mathrm{d}\Omega. \tag{12}$$

1.2 Derivating the functional J

The functional of the boundary value problem (2) is

$$J(\phi) = \frac{1}{2} a(\phi,\phi) - l(\phi) = -\frac{1}{2} a(\phi,\phi), \tag{13}$$

where ϕ is the unique solution of the variational equation $a(\phi, v) = l(v), \ \forall v \in W^1(\Omega)$. The derivative of the bilinear form a was computed, and is given in equation (12). The derivative of the functional J with respect to the domain, in the direction θ can therefore be evaluated.

$$J'(\theta) = -\frac{1}{2} a'(\phi,\phi)(\theta). \tag{14}$$

1.3 Rewriting a'

The derivative with respect to the domain Ω is defined through the vector field θ. We are *more precisely* interested in the derivative of J with respect to the *contact line* Γ. The vector field θ will only be non-zero in the neighbourhood of Γ.

Since the final aim is to study the influence of a deformation of the contact line Γ, and since the behaviour of the solution ϕ is *singular* around Γ, particular attention must be paid to the neighbourhood of Γ. In a way similar to the residue theorem, it seems natural to build some kind of half torus $\mathcal{T}_\varepsilon$ (like a *guttering*), of radius ε, around the contact line. The domain inside the half torus is called Ω^i_ε, and the domain outside Ω^o_ε, such that

$$\Omega = \Omega^i_\varepsilon \cup \Omega^o_\varepsilon, \text{ and } \Omega^i_\varepsilon \cap \Omega^o_\varepsilon = \emptyset. \tag{15}$$

The geometries of the considered domains are described in figure 2.

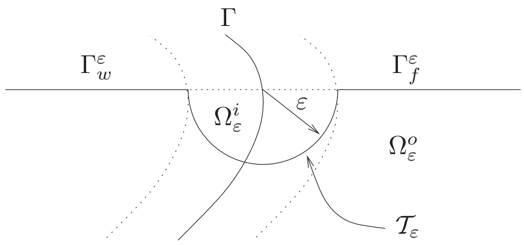

Figure 2: Two dimensional slice of the half torus, around the contact line Γ. The surface of the half torus $\mathcal{T}_\varepsilon$ defines the inside domain Ω^i_ε and the outside domain Ω^o_ε.

After some computation, we can write $a'(\phi,\phi)(\theta)$ as

$$\begin{aligned} a'(\phi,\phi)(\theta) = & \int_{\Omega^i_\varepsilon} div(\theta) \cdot |\nabla\phi|^2 \, \mathrm{d}\Omega \\ & -2 \int_{\Omega^i_\varepsilon} \nabla\phi \cdot \nabla\theta \cdot \nabla\phi \, \mathrm{d}\Omega \\ & + \int_{\partial\Omega^o_\varepsilon} |\nabla\phi|^2 \theta \cdot n \, \mathrm{d}\Sigma \\ & -2 \int_{\partial\Omega^o_\varepsilon} (\nabla\phi \cdot n) \cdot (\nabla\phi \cdot \theta) \, \mathrm{d}\Sigma. \end{aligned} \tag{16}$$

It is relevant to notice that the derivative $a'(\phi,\phi)(\theta)$ has been expressed as a sum of integrals on the boundary $\partial\Omega^o_\varepsilon$ of the domain Ω^o_ε, and on the inside domain Ω^i_ε. No integral on the outside domain Ω^o_ε remains.

Close to the contact line Γ, it is appropriate to decompose the displacement potential as the sum of a singular ϕ^S part and a regular part ϕ^R.

$$\phi = \phi^S + \phi^R. \tag{17}$$

The *local behaviour* of the singular part is *known.* In the local polar coordinate system around Γ, for any point

M of the contact line Γ, we express the singular part of the potential at any point $M' = (M, r, \vartheta)$ close to Γ.

$$\phi^S(M') = \phi^S(M, r, \vartheta) = K_\phi(M)\sqrt{r}\cos\frac{\vartheta}{2}, \tag{18}$$

where r is the distance of M' to the point M of the line Γ, and K_ϕ is the singularity cœfficient of the potential. For any given vector field θ under the previous assumptions, the limit of $a'(\phi, \phi)(\theta)$ as the radius ε of $\mathcal{T}_\varepsilon$ tends to zero may be computed.

$$a'(\phi,\phi)(\theta) \xrightarrow[\varepsilon\to 0^+]{} \frac{\pi}{4}\int_{M\in\Gamma} K_\phi^2(M)\cdot (\theta(M)\cdot n(M))\, \mathrm{d}\Gamma, \tag{19}$$

where n is the normal to Γ, in the plan $\{z = 0\}$, toward the outside of Γ.

It is then possible to define the derivative of the functional J with respect to the contact line. Substituting the limit of $a'(\phi, \phi)(\theta)$ in (14),

$$\frac{\partial J}{\partial \Gamma}(\theta) = -\frac{\pi}{8}\int_{M\in\Gamma} K_\phi^2(M)\cdot(\theta(M)\cdot n(M))\,\mathrm{d}\Gamma. \tag{20}$$

1.4 Intermediate conclusions

For *smooth* entering structures, the displacement potential is the *only* function for which the coefficient K_ϕ is zero all along the contact line. This relation expresses that *the displacement of the fluid is continuous*.

Thus, it can be deduced from equation (20) that the displacement potential will be the unique function for which $\partial_\Gamma J = 0$. The Wagner problem is to

$$\text{find } \Gamma \text{ such that } \frac{\partial J}{\partial \Gamma} = 0. \tag{21}$$

Since $\partial_\Gamma J \leqslant 0$ for every curve Γ, and since the Wagner solution is obtained for $\partial_\Gamma J = 0$, the Wagner problem can also be seen as an *unconstrained non linear* optimisation problem on Γ:

$$\Gamma = \arg\min_\Gamma \left|\frac{\partial J}{\partial \Gamma}\right|. \tag{22}$$

Because of numerical imprecision (space discretisation with elements, numerical integration, etc.), exact equality like in equation (21) may not be possible, leading to a *numerically* ill posed problem.

Moreover, in *two dimensions*, it is possible to describe exactly the contact line Γ *i.e.* the left and right points. But in *three dimensions*, for most general cases, the whole curve can only be *approximated*, hence the impossibility to reach exactly $\partial_\Gamma J = 0$.

It should then be better to consider the problem under its optimisation form (22).

2 A two dimensional example

In order to illustrate the previous section, the method is tested on an academic case, an inclined parabolic wedge. The selected shape for the parabolic wedge is $y = p(x) = \frac{1}{10}x^2$. The inclination angle is 4°. The chosen penetration depth is at $h = \frac{1}{100}$.

For this precise situation, the two contact points are

$$\begin{aligned} a_w &\simeq 0.4867, \\ b_w &\simeq 0.4145. \end{aligned} \tag{23}$$

The value of the functional J as a function of a and b is plotted in figure 3. This plot shows an horizontal tangent

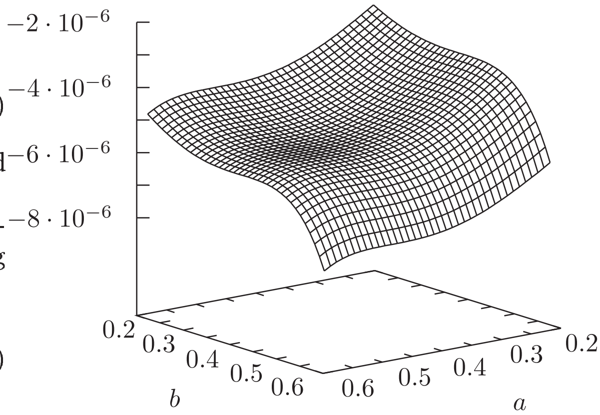

Figure 3: The functional J as a function of a and b.

plan around the point (a_w, b_w), illustrating the relation $\partial_\Gamma J \equiv 0$ of equation (21) for the Wagner solution.

Figure 4 plots the solutions of the two optimisation problems

$$\max_{a\in\mathbb{R}} \frac{\partial J}{\partial a}(a,b) \text{ and } \max_{b\in\mathbb{R}} \frac{\partial J}{\partial b}(a,b). \tag{24}$$

The intersection of the solution sets of these two equations is the point that maximises $\partial_a J + \partial_b J$. It also minimises the norm of $\|\partial_\Gamma J\| \equiv \left(\partial_a J^2 + \partial_b J^2\right)^{1/2}$. Its minimum $6.23\cdot 10^{-8} \neq 0$ is obtained for $(0.4868, 0.4146)$. Very good accordance is reached.

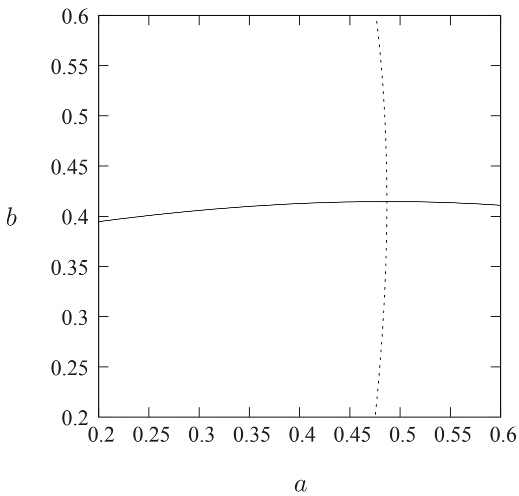

Figure 4: The dashed line is the solution set of the one dimensional minimisation problem $\min_{a\in\mathbb{R}} |\partial_a J|$. The thick line is the solution set of $\min_{b\in\mathbb{R}} |\partial_b J|$. The intersection of these two curves occurs at the point (a_w, b_w).

3 A three dimensional example

We use in this section the shape optimization technique on a three-dimensional example, the elliptic paraboloïd $z = 4x^2 + y^2$, for a penetration depth of 0.1. One of the interest of this test case is that the contact line is elliptic (see [SK01]); thus it can be described by two parameters, a and b, the semi-axes of the ellipse.

$$\begin{cases} x(\lambda) & = & a \cdot \cos(\lambda) \\ y(\lambda) & = & b \cdot \sin(\lambda) \end{cases} \tag{25}$$

For any given elliptic contact line, it is possible to compute the functional J. Figure 5 presents the values J as a function of the ellipse parameters a and b.

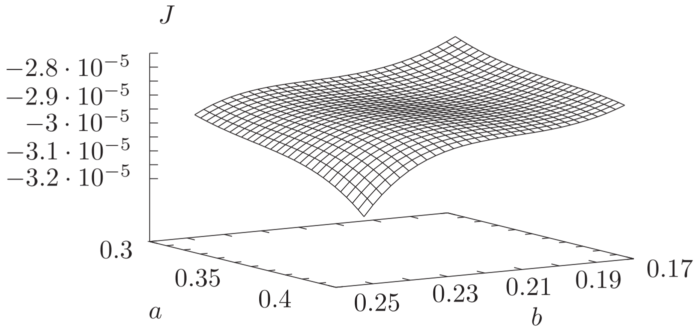

Figure 5: The functional J as a function of the semi axes a and b of the elliptic contact line Γ.

As performed for the two-dimensional inclined parabola, figure 6 plots the solution sets of $\max_{a \in \mathbb{R}} \partial_a J(a, b)$ and $\max_{b \in \mathbb{R}} \partial_b J$. The derivatives of J are computed using a centred finite difference approximation. The optimum is obtained for $a \simeq 0.2065$ and $b \simeq 0.3609$. These numerical results may be compared with the analytical solution $(0.2069, 0.3588)$ (see [SK01]).

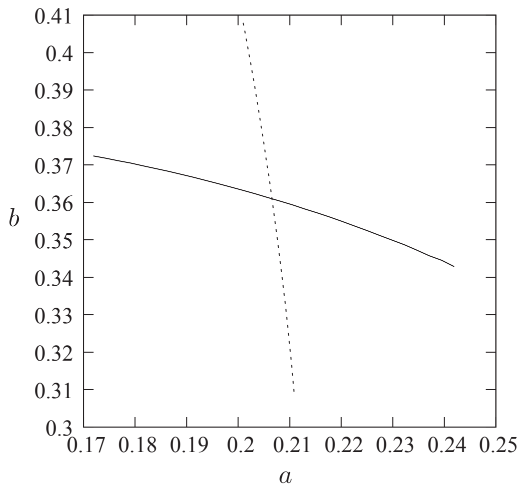

Figure 6: The dashed line is the solution set of the one dimensional minimisation problem $\min_{a \in \mathbb{R}} |\partial_a J|$. The thick line is the solution set of $\min_{b \in \mathbb{R}} |\partial_b J|$.

4 Conclusions

A link has been established between the singularity cœfficients of the potential and the variations of the functional J with respect to the contact line Γ.

For the particular case of the two dimensional impact, a 2 degrees of freedom[3] unconstrained optimization problem is set. The method has been illustrated on the numerical example of an inclined parabolic wedge.

In three dimensions, the method has been applied on an elliptic paraboloïd, showing good agreement with the analytical results.

References

[All06] G. Allaire. *Conception optimale de structures*, volume 58 of *Mathématiques et Applications.* Springer, 2006.

[GKMS05] T. Gazzola, A.A. Korobkin, S. Malenica, and Y.-M. Scolan. Three-dimensional Wagner problem using variational inequalities. In *proceedings of the International Workshop on Water Waves and Floating bodies*, volume 20, 2005.

[Kor82] A.A. Korobkin. Formulation of penetration problem as a variational inequality. *Din. Sploshnoi Sredy*, 58:73–79, 1982.

[SK01] Y.-M. Scolan and A.A. Korobkin. Three-dimensional theory of water impact. part 1. inverse Wagner problem. *Journal of Fluid Mechanics*, 440:293–326, 2001.

[Wag32] H. Wagner. Über Stoß-und Gleitvorgänge an der Oberfläche von Flüssigkieten. *Zeitschrift für Angewandte Mathematik und Mechanik*, 12:192–215, 1932.

[ZF93] R. Zhao and O.M. Faltinsen. Water entry of two-dimensional bodies. *Journal of Fluid Mechanics*, 246:593–612, 1993.

[3] The left and right contact points.